Raman spectroscopy of nanostructured silicon fabricated by metal-assisted chemical etching

Conference Paper *in* Proceedings of SPIE - The International Society for Optical Engineering · May 2014

DOI: 10.1117/12.2051489

6 authors, including:

Igor Iatsunskyi
Adam Mickiewicz University
102 PUBLICATIONS **912** CITATIONS
SEE PROFILE

Stefan Jurga
Adam Mickiewicz University
342 PUBLICATIONS **3,525** CITATIONS
SEE PROFILE

V. Smyntyna
Odessa National University
310 PUBLICATIONS **1,292** CITATIONS
SEE PROFILE

Mykola Pavlenko
15 PUBLICATIONS **148** CITATIONS
SEE PROFILE

Raman spectroscopy of nanostructured silicon fabricated by metal-assisted chemical etching

Dr. PhD Igor Iatsunskyi*[, 1, 2], Prof. Stefan Jurga[1], Prof. Valentyn Smyntyna[2], Mykolai Pavlenko[2], Valeriy Myndrul[2], Anastasia Zaleska[2]

[1]Nanobiomedical Center, Adam Mickiewicz University in Poznan
ul. Umultowska 85, PL 61614 Poznań, Poland

[2]Department of Experimental Physics, Odessa I.I. Mechnikov National University,
Str. Pastera 42, 65023, Odessa, Ukraine, yatsunskiy@gmail.com

ABSTRACT

In this work, we present a detailed experimental Raman investigation of nanostructured silicon films prepared by metal-assisted chemical etching with different nanocrystal sizes and structures. Interpretation of observed one and two-phonon Raman peaks are presented. First-order Raman peak has a small redshift and broadening. This phenomenon is analyzed in the framework of the phonon confinement model. Second-order Raman peaks were found to be shifted and broadened in comparison to those in the bulk silicon. The peak shift and broadening of two-phonon Raman scattering relates to phonon confinement and disorder. A broad Raman peak between 900-1100 cm^{-1} corresponds to superposition of three transverse optical phonons ~2TO (X), 2TO (W) and 2TO (L). Influence of excitation wavelength on intensity redistribution of two-phonon Raman scattering components (2TO) is demonstrated and preliminary theoretical explanation of this observation is presented.

Keywords: nanosilicon, metal-assisted chemical etching, Raman spectroscopy

1. INTRODUCTION

In recent years, silicon nanostructures have been extensively studied both theoretically and experimentally to realize their possible applications. For instance, silicon nanowires (Si NWs) exhibit novel chemical and physical properties due to their dimensions at the nano-scale, and offer great potential in the fields of electronics, photonics, chemical sensors and biological systems [1-3]. Nanostructured silicon is presently of widespread interest because Si is an extremely promising material not only for electronics but optoelectronics and solar cells [4-6].

Raman scattering has become a standard tool to study the silicon and nanostructured silicon for many years [7-10]. Raman-scattering studies of nanomaterials give us information about energy dispersion, structure, bonding and disorder. The analysis of nanostructures is mainly based on the phonon confinement model in which the finite crystallite size is taken into account by weighting the phonon-scattering efficiency. Confinement effects in nanostructures lead to modifications of the electronic, optical and vibrational properties. Unfortunately, if a first-order Raman spectrum of nanocrystalline silicon has been studied extensively, the second-order Raman scattering is investigated marginally [11, 12]. In the second-order Raman scattering process, two phonons of equal and opposite momentum participate and produce either line or broad continuous spectrum. Zone edge phonons, which appear only in higher-order Raman scattering, correspond to large wave vectors and are sensitive to short-range disorder. The nature of a material, such as crystalline or amorphous, can therefore be ascertained by analyzing the higher-order phonons as well. Study of second-order Raman scattering, in addition to first-order spectra, provides important information on the vibrational modes, energy structure, and morphology of nanostructured materials. Besides, second-order Raman scattering exhibits a higher sensitivity to nanoparticles size than first-order scattering [11].

*yatsunskiy@gmail.com; phone +380 673660744

Optical Micro- and Nanometrology V, edited by Christophe Gorecki, Anand Krishna Asundi, Wolfgang Osten, Proc. of SPIE Vol. 9132, 913217 · © 2014 SPIE
CCC code: 0277-786X/14/$18 · doi: 10.1117/12.2051489

In this paper we present the one- and two-phonon Raman spectra of nanostructured silicon fabricated by metal-assisted chemical etching. We have measured the Raman frequency shifts and line shapes at room temperature. We focused on the changes in the second-order Raman scattering. New effect dealing with second-order Raman scattering was found.

2. EXPERIMENTAL

The nanostructured silicon samples were fabricated utilizing a metal-assisted chemical etching process (MACE) [13]. The MACE exhibits good process controllability to generate various nanostructured silicon surface morphologies. Similar to electrochemical etching to create porous silicon, MACE acts as a localized electrochemical etching process in which local electrodeless etching occurs at the metal/silicon interface, each nanometer-sized metal particle acts as a local cathode and the silicon surface acts as an anode. The metal particles are critical in the process to promote H_2O_2 decomposition and cause electron–hole injection into the silicon surface; silicon is dissolved by HF to create pits or other nanostructures on the surface.

Monocrystalline silicon samples with different resistivity, orientation and type after standard RCA cleaning, were cleaned with acetone/isopropanol and deionized water via ultrasonic cleaning. The silver particles, which act as catalysts to assist the etching of silicon, were deposited on Si samples by immersion in metallization aqueous solutions of $AgNO_3$ with different silver concentration. After the electroless metallization, the wafers were etched in aqueous solutions containing HF (40%), H_2O_2 (30%), and ultrapure H_2O at various ratio concentration. After etching, the samples were etched in HNO_3 solution to remove silver particles and then were cleaned with deionized water and blown dry with nitrogen. The etching and immersion procedures were performed at room temperature.

To investigate the structure of the layers Jeol 7001TTLS scanning electron microscope and Atomic Force Microscope (Bruker company) BioScope Catalyst microscope were used. In the last case, the measurements were carried out in the contact mode. The radius of curvature of the silicon nitride probe was 10 nm.

Raman scattering measurements were performed using a Renishaw micro-Raman spectrometer equipped with a confocal microscope (Leica). The samples were measured in backscattering geometry with a spectral resolution better than 1.0 cm^{-1}. The incident light was not polarized; also the detection setup contained no polarization filters The Raman scattering spectra were excited by 488 nm, 514 nm and 633 nm. The beam was focused on the samples with a 50 x microscope objective with a numerical aperture of 0.4. The incident optical power was changed by using neutral density filters in the beam path. The minimum power for which a signal could be measured was limited by the signal to noise resolution of the detector in the spectrometer. All measurements were performed at room temperature in ambient atmosphere.

3. RESULTS AND DISCUSSIONS

Figs. 1 (A)–(D) are the images of scanning electron microscopy, which show the surface morphology of nanostructured silicon samples fabricated by MACE. The n-type samples (100 orientations) with resistivity 4.5 Ohm cm show (Figs. 1(A)–(B)) mostly the porous structure. This morphology shown in images indicates pores of different sizes depending on the chemical procedures. Pore depth was a few hundred nanometers, not as large as the diameter. On the other hand, AFM studies of that samples show the presence of nanometer-sized pyramids (hillocks) between the macropores. These hillocks apparently correspond to Si nanocrystallites, whereas the hollows between them correspond to the narrow (nanometer) pores on the surface. The lateral dimensions of the hillocks, which were determined from cross-sections of AFM images as their largest linear dimensions at a base, are in the range of 15–45 nm. The sizes of hillocks increase down to the bottom of pores. It should be noted that the actual lateral dimensions of the elements of the structure are smaller than the dimensions of the AFM images by approximately the doubled radius of the probe tip.

P-type samples with resistivity 80 Ohm cm (Figs. 1(C)–(D)) have mostly the “coral-like” structure similar to nanowires with different orientation. Wires have approximate dimensions lying in the range of 10–50 nm. AFM shows mostly the cauliflower-like structure. This morphology shown in 2D images indicates several particles (granules) embedded in each grain. However, the shapes, as well as arrangement of the grains, were found to be different.

All these results confirm that different morphologies can be produced by varying either the dopant level and, of course, the type of etchant and deposition solution.

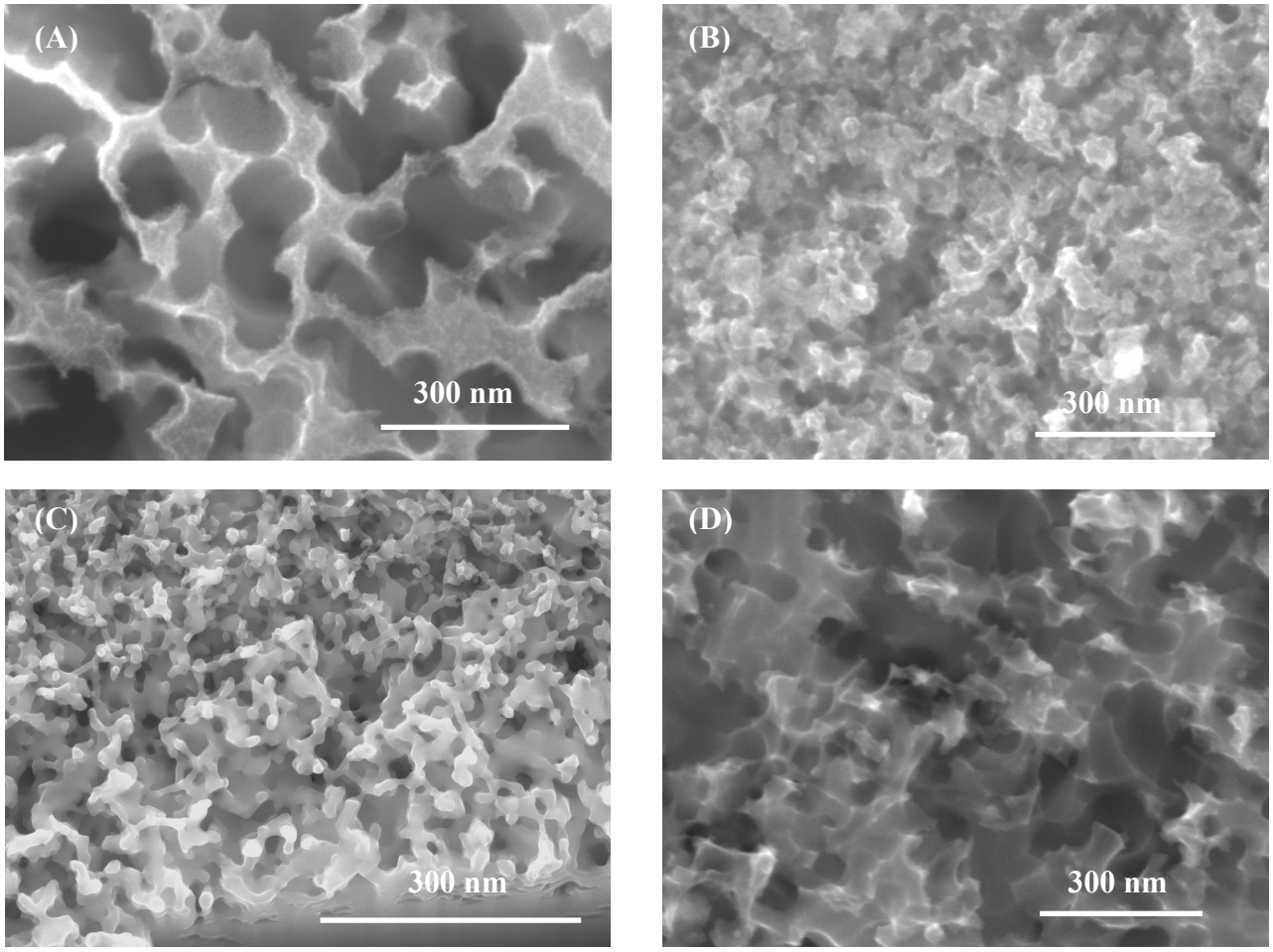

Fig.1. Ag particles were deposited on Si samples by immersion in 0.23 M HF and 10^{-3} M $AgNO_3$ metallization aqueous solutions. The time of immersion was varied – 40 s. for samples (A) and sample (C); and 200 s. for sample (B) and sample (D). Etching solution contained HF (40%), H_2O_2 (30%), and ultrapure H_2O at ratio concentration - $H_2O_2/H_2O/HF$=10/80/40, for 30 minutes.

Under normal conditions (standard pressure and temperature), silicon crystallizes in a diamond lattice structure, which belongs to the O_n^7 space group. The diamond structure of silicon allows only one first-order Raman active phonon of symmetry Γ_{25} located at the Brillouin zone (BZ) centre corresponding to a phonon wavevector 520.0 ± 1.0 cm^{-1} with the full width at half maximum (FWHM) – 3.5 cm^{-1}.

Raman scattering spectra of sample (A) is shown in Fig.2. High peak at 517-519 cm with the FWHM of 8-12 cm^{-1} can be seen in the Raman spectrum of nanostructured Si. The intensity of the first-order scattering which is due to the optical phonons (TO, LO) at the center Γ point of the BZ, as was mentioned above, is much stronger in comparison with that from the initial Si wafer. In comparison with the first-order optical phonon peak of *c*-Si, the corresponding Raman peak of nano-Si has frequency down-shifted, its linewidth broadened and its line shape becomes asymmetric with a little tail on the low-energy side extending to 470-480 cm^{-1} for all samples what indicate on amorphous-like structure. The first-order spectrum from bulk Si single crystal represents scattering by optical phonons with quasimomentum **q**=0 because of its conservation in an infinite lattice. Studies of the morphology and structure of nano - Si by SEM and AFM have revealed the presence of nanostructures with dimensions on a nanometer scale (Fig. 1). The limitation of the translation symmetry leads to relaxation of this selection rule, and phonons with quasimomentum out of the region around the Γ point determined by the size of the crystallite can contribute to the scattering. Due to the decrease in the frequency of optical phonons with **q** in the vicinity of the BZ center, the Raman line of a spectrum from nanocrystalline material is shifted to lower energies and broadened. But comparing our experimental data with references one should conclude that there are additional reasons of the red-shifting and broadening. Analyzing results of many publications we can conclude that the main mechanism of Raman shift and broadening is confinement effect.

Campbell and Fauchet [14] developed a quantitative model that calculates the Raman spectrum of porous silicon as depending on the size L and on the shape of the porous silicon crystallites. If PS is modelled as an assembly of quantum wires, the phonon confinement is assumed to be two dimensional, while if the PS is modelled as an assembly of quantum dots, the confinement is three dimensional. The Raman spectrum is given by:

$$I(\omega) \cong \int_{BZ} \frac{d^3q\,|C(0,q)|^2}{(\omega-\omega(q))^2-(\frac{\Gamma_0}{2})^2}; \quad (1)$$

where

$$|C(0,q)|^2 = \exp(-\frac{q^2L^2}{16\pi^2}); \quad (2)$$

The first-order Raman spectrum $I(\omega)$ is thus given by:

$$I(\omega) \cong \int_{BZ} \frac{4\pi q^2 \exp(-\frac{q^2L^2}{16\pi^2})d^3q}{(\omega-\omega(q))^2-(\frac{\Gamma_0}{2})^2}; \quad (3)$$

where Γ_0 is the natural linewidth for c-Si at room temperature and $\omega(q)$ is the dispersion relation for optical phonons in c-Si. This expression can be taken as [14]:

$$\omega = \omega_0 - 120\,(\frac{q}{q_0})^2; \quad (4)$$

Here, ω_0 is the position of the c-Si Raman peak. By specifying the size of the silicon nanocrystallites, from eqs. (3) and (4) the relation between the peak shift and the linewidth in the framework of the phonon confinement model can be determined. The results of calculations are presented in Fig. 3.

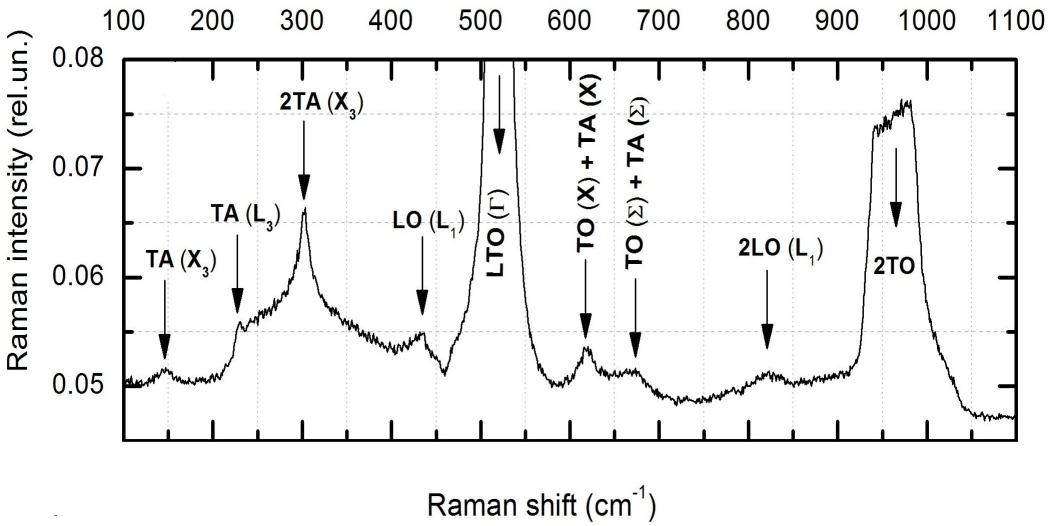

Fig.2. Normalized Raman spectrum of Si nanostructures taken with a 514 nm laser. (A) sample.

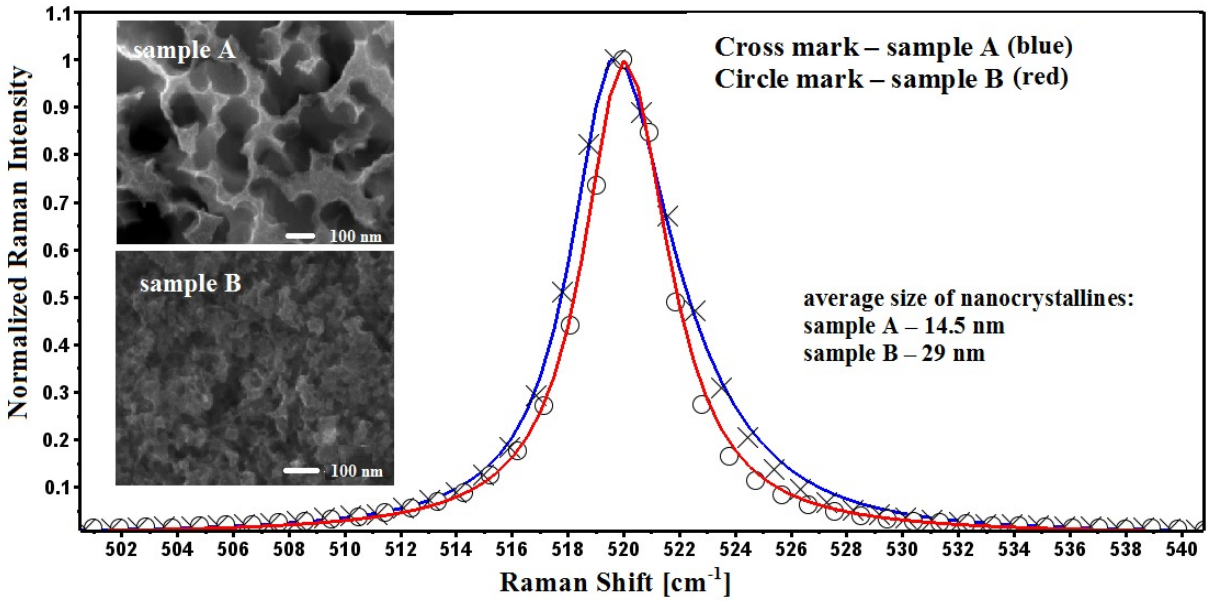

Fig. 3. Experimental and calculated curves of nanostructured silicon surface.

In contrast to c-Si, one can see the first-order scattering from acoustical phonons at 150 cm^{-1} and optical phonon at 430 $cm^{-1.}$ These peaks correspond to TA phonon at *X* critical points – TA (X) and to LO phonon at L critical points –LO (L), respectively. The last peak suggests that nanostructured silicon in some extent is in amorphous form [15].

A strong enhancement of multiphonon features occurs for nanostructured silicon. The second order spectrum is much weaker than the first-order peak LTO (Γ) with features ranging from 100–1100 cm^{-1}. The second-order spectrum of transverse 2TA acoustical phonons is clearly observed near 300 cm^{-1}. Some authors suggest this peak is corresponding to LA modes [16] but there is not accurately confirmation of this fact. Probably we observe the superposition of transverse and longitudinal acoustic modes. Comparing the peak position with the values in the table 1, we can assume that this peak corresponds to TA overtones at *X* critical points – 2TA (X). We can also observed few little two-phonon peaks - 2TA (L) at 230 cm^{-1} and 2LO (L) at 830 cm^{-1}. Some authors explain the 2LO (L) by some kind of disorder but it still is open question [17]. In addition, we also found two obvious peaks of Si nanocrystallines at 630 and 670 cm^{-1} which can be ascribed to the quantum confinement effect of Si. These peaks are composed of contributions from combinations and also from overtones of transverse optical and acoustical modes of different critical points. The peak at 630 cm^{-1} probably corresponds to the combination TO (X) +TA (X) modes and weaker peak corresponds to TO (Σ) +TA (Σ). Probably, longitudinal modes are also taking part in these combinations as indicated in some publications [18]. And finally, there is a broad peak between 900-1100 cm^{-1} which is from the scattering of few transverse optical phonons ~2TO phonons (Fig.4). To date, there is no consensus about the origin of the broad peak. Some authors argue that this peak is formed by the superposition of two or more optical modes [10-18]. It can be seen that shape line has a kind of complexity. By means of Origin pro software, the Raman peak was split onto separate peaks. The peaks, located at 930-940, 950-960 and 980-985 cm^{-1} have been found. The shoulder at 930-940 cm^{-1}, which is identified as two-TO-phonon overtone at zone-edge point X, emerges at 930 cm^{-1} – 2TO (X). The peak at 945-955 cm^{-1}, which is identified as two-TO-phonon overtone at zone-edge point W, emerges at 940 cm^{-1} – 2TO (W). Furthermore, the peak at 980 cm^{-1} corresponding to 2TO-phonon overtone scattering from the critical point L, appears at 980 cm^{-1} – 2TO (L). It was noticed that the 2TO peaks narrow as the size of the nanostructures become larger. It is clear from these results that the 2TO band is affected by confinement effects and shifts towards lower frequency and becomes broader as the dimension of the nanocrystals decreases.

Exploring the patterns of change in this peak, depending on the wavelength of the excitation light (λ_{exc}) we found an interesting effect. Changing the λ_{exc} leads to an intensity redistribution of Raman scattering components. One can notice that for λ_{exc}=488 nm and λ_{exc}=514 nm the peaks of 2TO (L) and 2TO (W) prevail over the 2TO (X) mode. For the λ_{exc}=633 nm 2TO (X) phonon overtone comes maximum and the left shoulder of the broad peak becomes much higher than right shoulder. In order to explain this effect we considered following assumptions: increasing in the intensity of the second-order Raman scattering depends on Raman tensor and effective Raman scattering cross-section. On the other hand, the Raman tensor depends on the probability of interband optical transitions [19]. Photons with energies

corresponding to the absorption edge for a certain zone-edge point of BZ should have a higher probability of optical transitions and thereby the intensity of Raman peak for certain zone-edge point would increase or decrease its value. However, the present explanations are tentative, and require further theoretical proof.

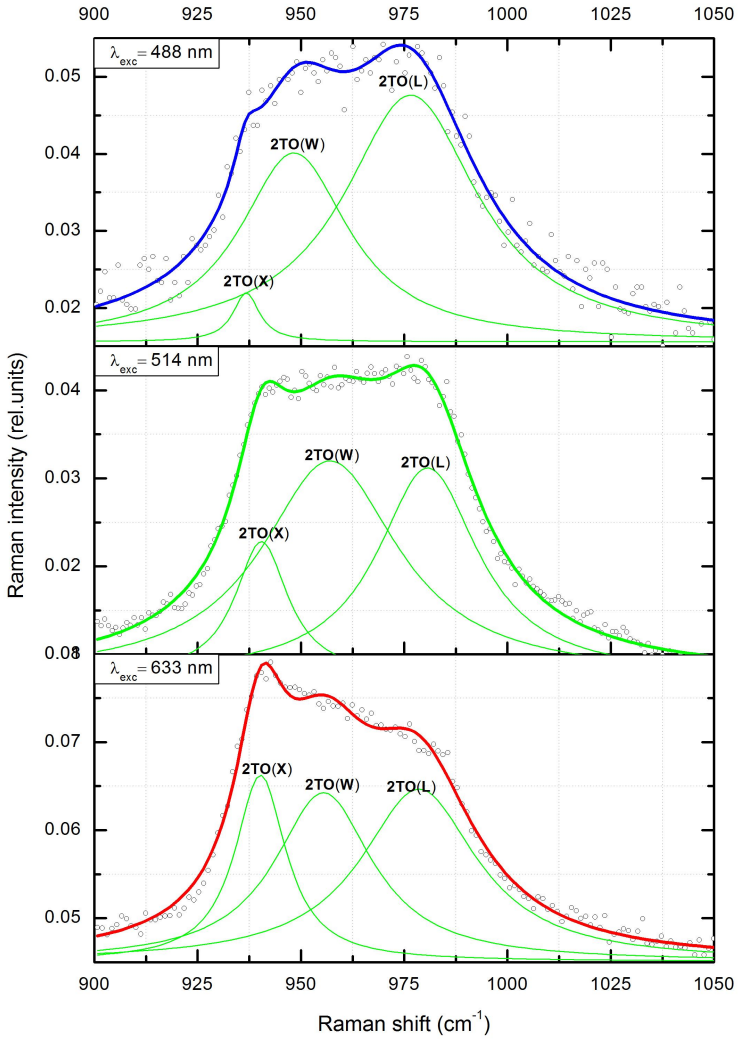

Fig. 4. Normalized Raman two-phonon scattering for three different laser wavelengths for sample (C). The calculated separate second-order modes are indicated by solid green line curve and the experimental data are plotted as colored bold line.

4. CONCLUSION

One- and two-phonon Raman scattering characteristics of nanostructured silicon fabricated my metal-assisted chemical etching were investigated and the results are summarized. First-order Raman peak has a redshift and broadening compared with bulk silicon as predicted by the phenomenological phonon confinement effect for nanostructures. In addition to the fundamental phonon modes, overtone and combinations of modes were also observed and analyzed. Second-order Raman peaks were found to be shifted and broadened in comparison to those in the bulk silicon. A broad peak between 900-1100 cm^{-1} corresponds to superposition of three transverse optical phonons ~2TO (X), 2TO (W) and 2TO (L). It was observed the anomalous behavior of the 2TO peaks depending on the wavelength of the excitation light. Our findings are important for characterizing of nanostructures by Raman scattering.

REFERENCES

[1] Bisi, O.; Ossicini, S.; Pavesi, L., "Porous silicon: A quantum sponge structure for silicon based optoelectronics," Surf. Sci. Rep., vol. 38, 1-126 (2000).

[2] Pavesi, L.; Turan, R., [Silicon Nanocrystals. Fundamentals, Synthesis and Applications], Wiley-VCH: Weinheim, Germany, 349-394 (2010).

[3] Igor Iatsunskyi, Valentyn Smyntyna, Mykolai Pavlenko et. al., "Ammonia detection using optical reflectance from porous silicon formed by metal-assisted chemical etching," Proc. SPIE. 8901, Optics and Photonics for Counterterrorism, Crime Fighting and Defence IX; and Optical Materials and Biomaterials in Security and Defence Systems Technology X, 89010K. (October 16, 2013).

[4] Igor Iatsunskyi, Valentin Smyntyna, Nykolai Pavlenko, and Olga Sviridova, "Peculiarities of Photoluminescence in Porous Silicon Prepared by Metal-Assisted Chemical Etching," ISRN Optics, Article ID 958412, 6 pages (2012).

[5] L.Y. Cao, J.S. White, J.S. Park et.al., "Engineering light absorption in semiconductor nanowire devices", Nat. Mater., Vol. 8, 643 (2009).

[6] S.E. Han, G. Chen, "Optical Absorption Enhancement in Silicon.Arrays for Solar Photovoltaics", Nano Lett., Vol. 10, 1012-1015, (2010).

[7] T. Kamiya, M. Kishi, A. Ushirokawa, T. Katoda, "Observation of the amorphous-to-crystalline transition in silicon by Raman scattering", Appl. Phys. Lett., vol. 38(5), 377-379, (1981).

[8] Min Yang, Darning Huang, Pinghai Hao, et. al., "Study of the Raman peak shift and the linewidth of light-emitting porous silicon", J. Appl. Phys., vol.**75**(1), 651-653, (1993).

[9] H. Tanino, A. Kuprin, H. Deai, "Raman study of free-standing porous silicon", Phys. Rev. B, vol. 53(4), 1937-1947, (1996).

[10] Bibo Li, Dapeng Yu, Shu-Lin Zhang, "Raman spectral study of silicon nanowires", Phys. Rev. B, vol. 59(3), 1645-1648, (1999).

[11] Rong-ping Wang, Guang-wen Zhou, Yu-long Liu, et. al., "Raman spectral study of silicon nanowires: High-order scattering and phonon confinement effects", Phys. Rev. B, vol. 61(24), 16827-16832, (2000).

[12] Puspashree Mishra, K. P. Jain, "First- and second-order Raman scattering in nanocrystalline silicon", Phys. Rev. B vol.64(7), 073304-073308, (2001).

[13] Z. Huang, N. Geyer, P. Werner, J. De Boor, and U. Gösele, "Metal-assisted chemical etching of silicon: a review," Advanced Materials, vol. 23, no. 2, 285–308 (2011).

[14] I. H. Campbell and P. M. Fauchet, "The effects of microcrystal size and shape on the one phonon Raman spectra of crystalline semiconductors", Solid State Communications, vol. 58, 739-741, (1986).

[15] Mile Ivanda, Ozren Gamulin, Wolfgang Kiefer, "Mechanism of Raman scattering in amorphous silicon", Journal of Molecular Structure, vol.480–481, 651–655, (1999).

[16] Wensheng Wei, "One- and two-phonon Raman scattering from hydrogenated nanocrystalline silicon films", Vacuum, vol.81, 857–865, (2007).

[17] Wensheng Wei, Gangyi Xu, Jinliang Wang, Tianmin Wang, "Raman spectra of intrinsic and doped hydrogenated nanocrystalline silicon films ,Vacuum, vol.81, 656–662, (2007).

[18] Dorra Abidi, Bernard Jusserand, Jean-Louis Fave, "Raman scattering studies of heavily doped microcrystalline porous silicon",Phys. Rev. B, vol.82(7), 075210-075221, (2010).

[19] M Khorasaninejad, J Walia, S Saini, "Enhanced first-order Raman scattering from arrays of vertical silicon nanowires", Nanotechnology, vol.23, 275706- 275713, (2012).